Published in final edited form as:
*J Appl Physiol*. 2007 July ; 103(1): 240–248.

# VERTICAL GRADIENTS IN REGIONAL LUNG DENSITY AND PERFUSION IN THE SUPINE HUMAN LUNG: THE SLINKY® EFFECT

**Susan R. Hopkins**[1,2], **A. Cortney Henderson**[1], **David L. Levin**[2], **Kei Yamada**[3], **Tatsuya Arai**[1], **Richard B. Buxton**[2], and **G. Kim Prisk.**[1,2]

1 *Department of Medicine, University of California, San Diego, La Jolla CA, 92093*

2 *Department of Radiology, University of California, San Diego, La Jolla CA, 92093*

3 *School of Medicine, University of California, San Diego, La Jolla CA, 92093*

## Abstract

*In-vivo* radioactive tracer and microsphere studies have differing conclusions as to the magnitude of the gravitational effect on the distribution of pulmonary blood flow. We hypothesized that some of the apparent vertical perfusion gradient *in-vivo* is due to compression of dependent lung increasing local lung density and therefore perfusion/volume. To test this, 6 normal subjects underwent functional MRI with arterial spin labeling during a breath-hold at functional residual capacity, and perfusion quantified in non-overlapping 15mm sagittal slices covering most of the right lung. Lung proton density was measured in the same slices using a short echo 2D-FLASH sequence. Mean perfusion was 1.7 ± 0.6 ml/min/cm$^3$ and was related to vertical height above the dependent lung (slope = −3%/cm, $p < 0.0001$). Lung density averaged 0.34 ± 0.08 g/cm$^3$, and was also related to vertical height (slope = −4.9%/cm, $p < 0.0001$). By contrast when perfusion was normalized for regional lung density, the slope of the height-perfusion relationship was not significantly different from zero ($p = 0.2$). This suggests that *in-vivo* variations in regional lung density affect the interpretation of vertical gradients in pulmonary blood flow and is consistent with a simple conceptual model: that the lung behaves like a Slinky®, a deformable spring distorting under its own weight. The greater density of lung tissue in the dependent regions of the lung is analogous to a greater number of coils in the dependent portion of the vertically oriented spring. This implies that measurements of perfusion *in-vivo* will be influenced by density distributions and will differ from excised lungs where density gradients are reduced by processing.

### Keywords

Functional magnetic resonance imaging; lung perfusion; lung density; gravity

## Introduction

The effect of gravitational forces on the distribution of pulmonary blood flow has been the subject of interest for some time, and the magnitude of that effect is the subject of active debate. More than 45 years ago, West and Dollery described gravitational differences in the uptake of radioactive carbon dioxide (45), a soluble perfusion-limited gas, which they used as a marker of regional perfusion in healthy humans. In that study of the upright lung during a breath-hold

Address for Correspondence: Susan R. Hopkins MD PhD, Associate Professor of Medicine and Radiology, Division of Physiology, Department of Medicine, University of California San Diego, 9500 Gilman Dr., La Jolla CA, 92093, 858-534-2680, Tel 858-534-4812, Fax shopkins@ucsd.edu.

Slinky® is a registered trademark of Poof-Slinky Inc.

at one liter above functional residual capacity, external counters recorded greater uptake of $CO_2$ in the dependent portions (base) of than in the non-dependent apices, consistent with greater blood flow in these regions. These finding were confirmed using $^{133}$Xenon (3), and later this gravitational effect was shown to be greater at high lung volumes (22). Subsequent measurements in humans in prone and supine postures using a variety of imaging techniques, such as positron emission tomography (5,29), single photon emission tomography (26), and magnetic resonance imaging (25) also demonstrate gravitational influences on pulmonary perfusion. In addition, studies using a hyperventilation-breathhold technique conducted in microgravity have shown that pulmonary blood flow becomes more uniform when gravitational forces are eliminated (34,41). These studies all suggest a substantial effect of gravity on the distribution of pulmonary perfusion in the human lung.

In contrast, although studies in animals using microspheres have demonstrated a gravitational influence on pulmonary perfusion (12,13,15), the data from these studies have shown that there is greater perfusion heterogeneity within an isogravitational plane than across gravity. This is a consistent finding in a variety of animal species, not only in quadrupeds such as horses (19) and pigs (14), but also in primates such as baboons who assume an upright posture (12). These studies suggest that gravitational influences account for only 1–25 % of the variability in regional perfusion, with the remainder being attributed to the influences of vascular structure (12,14,19).

That the lung has the potential to distort under its own weight has been discussed by many authors (3,23,24,36) particularly as it affects the distribution of ventilation and alveolar size. For example, in dog lungs frozen *in situ,* there are gravitationally dependent gradients in alveolar size (11), with smaller alveoli in dependent portions of the lung. Consistent with this, there are vertical gradients in lung density and, in the supine posture, the density of dependent regions of the lung is approximately 40% greater than the non-dependent portions of the lung (6). Chest radiographs obtained at total lung capacity, functional residual capacity, and residual volume during parabolic flight also show gravitational variation in regional lung density, with an increase in density in the upper lung zones at all lung volumes during microgravity (33) compared to 1G. However, the effect that non uniform lung density has on the measurement of the distribution of pulmonary perfusion using different techniques and on pulmonary perfusion itself has been less well described.

A common theme of lung perfusion measurements discussed above relates to the way in which perfusion is measured, either as flow per unit volume, or the lung as a whole. When the intact lung is sampled as with inert gas washout studies ($CO_2$ or $^{133}$Xenon), the precise volume of lung sampled is unknown, or in the case of positron emission tomography and magnetic resonance imaging, perfusion is measured as ml of blood/min/cm$^3$ of lung. Thus, for measurements made in intact human lungs, the effect of gravity on lung distortion and regional density is potentially important, as any compression of dependent lung regions will be reflected in measures of regional perfusion. This is because a given volume of lung in the dependent portion of the lung will contain more lung tissue (capillaries) and less air, and will thus have a greater density than in non-dependent regions. In addition, blood contained within the pulmonary circulation will provide additional deformation under gravity according to its distribution in the lung. This is not the case with perfusion measurements made with microspheres, since following the infusion of microspheres *in situ*, the lung is washed of blood, air dried and inflated to total lung capacity. Thus, any effects of lung distortion and non-uniform density present in the *in situ* lung due to gravity are lessened and the resulting measurements of microsphere location have the potential to underestimate any effect that regional variations in lung density, whether gravitationally-based or otherwise, will have on the measurement of perfusion (9).

Regional pulmonary perfusion can be quantified using high resolution magnetic resonance imaging techniques (4,18,20), as can regional proton (water) density (16). The application of these techniques in the lung has been recently reviewed (21). The importance of these high resolution (0.14 $cm^3$) techniques are that combined, they allow the effects of gravity on regional lung perfusion to be considered independently and virtually simultaneously from the effects on regional lung density.

The purpose of this study was to examine the combined vertical gradients in regional blood flow and lung density in the normal human lung. We obtained measures of regional lung perfusion per volume of lung, comparable to the original studies of West and Dollery (45). These measures include the distorting effects of gravity on the lung architecture. We also measured lung proton density in order to calculate perfusion per gram of lung water, to allow for variation of regional lung density. We hypothesized that the gravitationally based gradients in regional pulmonary perfusion would be reduced when the effects of density are considered, consistent with the discrepant results between microsphere and *in situ* data. The results of this study are consistent with a simple conceptual model: that the lung behaves like a Slinky ®, a deformable spring that distorts under its own weight.

## Methods

### Subjects

This study was approved by the Human Subjects Research Protection Program of the University of California, San Diego. Six healthy subjects (2 female, 4 male, age = 25 ± 1 years, weight = 73.6 ± 8.3 kg) participated after giving informed consent. Subjects underwent screening using pulmonary and MRI safety questionnaires, followed by a medical history and physical exam.

## Data collection

Each subject underwent MRI scanning using a Vision 1.5 T whole-body MR Scanner (Siemens Medical Systems, Erlangen, Germany). All sequence parameters were kept within U.S. Food and Drug Administration guidelines for clinical magnetic resonance examinations. Subjects were positioned supine in the scanner, with a custom designed rigid PVC tubing cage positioned over the torso. The phased-array torso coil was positioned on this frame ensuring a constant distance between the anterior and posterior elements of torso coil. A water phantom doped with gadolinium (Berlex Imaging, Magnevist®, 469 mg/mL gadopentetate dimeglumine, 1:5500 dilution) to $T_1$ and $T_2$ values approximating that of blood, was placed next to the subject within the field of view for absolute quantification of pulmonary perfusion and proton density (see below). Perfusion, proton density and coil correction data (all described below) were acquired by imaging the right lung in the sagittal plane, to eliminate artifact from the aorta and heart present within the left hemithorax. Sequential 15 mm slices were obtained in triplicate and a constant level of breath holding was ensured by overlaying sequential images from the same slice and visually inspecting for discrepant lung volumes, which were discarded. Data were acquired during a 8–10 second breath-hold at functional residual capacity starting in the medial lung adjacent to the heart and progressing laterally until signal intensity was reduced to less than 50% of baseline or until the imaging plane included the lateral chest wall. This was accomplished in 3–5 slices for each subject, depending on lung size. Of these, the middle three slices were selected for each subject, or in the case where 4 slices were obtained, data from the most lateral slice was not used.

### Correction for coil inhomogeneity

In order to maximize the signal to noise ratio in the pulmonary perfusion and proton density data (described below), a torso coil was used, which has substantially higher gain than the body coil built into the scanner. However, unlike the body coil, which is quite homogeneous, the torso coil exhibits a degree of inhomogeneity in signal strength that varies in all 3 directions. To correct for this inhomogeneity, the image signal obtained from the torso coil was corrected to the homogeneous (but noisy) body coil signal for each subject individually as follows: Fifteen mm thick 2D standard proton density images were acquired in the same slice location using a FLASH (Fast Low-Angle SHot) sequence (see below), one with the torso coil and one with body coil. Each of two images was smoothed by taking the 2D Fourier Transform, applying a Gaussian smoothing function, and transforming back into the image domain. The resultant images were heavily smoothed with a maximum spatial frequency across the field of view of ~2 cycles; approximately twice the spatial frequency of the torso coil elements (approximately a 5 cm resolution). The two smoothed images were divided to define the low spatial frequency coil sensitivity function, which was then multiplied by all images obtained using the torso coil on a voxel-by-voxel basis.

### Quantification of regional pulmonary perfusion with ASL

Regional pulmonary blood flow was assessed using a 2D ASL-FAIRER sequence with a half-Fourier acquisition single-shot turbo spin-echo (HASTE) imaging scheme. The 15-mm-thick sagittal slices has a field of view of 40cm × 40cm and a resolution of 256 × 128 pixels, therefore voxels of approximately 1.5 × 3 × 15 mm (~0.07$cm^3$) were obtained. These ASL image files were later resized during post-processing to match the voxel size of the FLASH proton density images (3 × 3 × 15mm, giving an effective resolution of ~0.14 $cm^3$) using bilinear interpolation in MATLAB (The MathWorks, Inc, Natick, MA). Once the subtracted ASL image was corrected for coil inhomogeneity, as described previously, pulmonary blood flow was quantified in ml/min/$cm^3$. Assuming that the water phantom and blood have matched $T_1$ and $T_2$ (the phantom is doped to achieve this) and the $T_1$ of lung at 1.5T is 1350 msec (28), then for a given R-R interval and inversion time (TI), pulmonary blood flow can be quantified from the subtracted ASL signal provided it is corrected to the signal resulting from the water phantom in the raw images. The quantified flow for each voxel was expressed in units of $mL_{blood}$/min/$cm^3{}_{lung}$ (averaged over a complete cardiac cycle). The technique for quantifying regional pulmonary perfusion was modified from one previously reported (30,32) to allow for acquisition of data within a single breath-hold (4). It has been recently described in detail (4, 21) and is therefore only briefly described here.

Arterial spin labeling exploits the capability of MRI to invert the magnetization of protons (primarily in water molecules) in a spatially selective way using a combination of radiofrequency pulses and spatial magnetic field gradient pulses. By inverting the magnetization of arterial blood, these "tagged" protons in blood act as an endogenous tracer. During each measurement two images are acquired during a single breath-hold of each lung slice with the signal of blood prepared in a different way. Then the two images are subtracted, canceling the stationary signal, to give a quantitative map of pulmonary perfusion (4). In the first image, termed the "tag" image, the magnetization of the arterial blood both inside and outside the imaged section is inverted at the beginning of the experiment with a preparatory inversion (180º) pulse applied to the whole lung (a spatially non-selective inversion). In the second "control" image, a preparatory inversion (180º) pulse is applied only to the section being imaged (a spatially selective inversion), leaving the arterial blood outside the imaged section undisturbed. In both images, a spatially selective 90º pulse is also applied to the imaged section immediately after the preparatory inversion pulse. The effect of these radio frequency pulses during the preparation phase is that the static magnetization within each voxel of the image plane is reduced to near zero in both experiments, but the blood magnetization outside

the imaging plane is fully inverted prior to the tag image but fully relaxed prior to the control image. In both cases, after a delay encompassing ~80% of one R-R interval, the images are acquired. During this delay blood flows into each voxel of the imaged section, and there is also relaxation of the magnetization. The static magnetization relaxes identically in both cases, so when the two images are subtracted this signal is cancelled.

In the tag image, the inverted magnetization of blood has relaxed part way to equilibrium, while for the control image the magnetization of blood outside the imaging plane remains fully relaxed (giving an strong MR signal). The difference signal (control – tag) measured for each voxel then reflects the amount of blood delivered during the interval TI, weighted with a decay factor due to the relaxation of the blood magnetization during that interval. In the ASL difference image (Figure 1A), the signal intensity for each voxel is proportional to the amount of blood delivered during one heart cycle (TI), and so is proportional to the local pulmonary blood flow expressed as ml/min/$cm^3$.

### Quantification of regional lung density

In addition to the ASL images, a proton density image was acquired in the same sagittal slice using a FLASH (Fast Low-Angle SHot) sequence during a separate breath-hold. Sequence parameters were repetition time (TR) = 6 msec, echo time (TE) = 0.9 msec, flip angle = 4°, slice thickness 15 mm, and image size 128 × 128. In each image so obtained, the resulting signal in each voxel, after correcting for coil inhomogeneity is related to the signal derived from the water phantom (which is by definition 100% water) to obtain regional lung proton (water) density in units of ml $H_2O$/$cc^3$ lung. The resulting proton density was then calculated by correcting the signal for the rapid T2* decay of signal from the lungs based on published values of T2* (1.43 ± 0.41 msec,(17)). For simplicity, this proton density which reflects both tissue and blood is subsequently referred to in this manuscript as density.

### Density corrected Perfusion

Perfusion expressed in units of ml/min/g lung can be approximated by dividing the image acquired by ASL, which has the units of ml/min/$cm^3$ lung, by the FLASH image of proton density (in g $H_2O$/$cm^3$ lung) to give perfusion in ml/min/g lung (tissue + blood). A mutual-information-based technique that included translation and rotation was utilized to register the two images (39), and the ASL image was divided by the FLASH image to give perfusion in ml/min/g using a custom designed program in MATLAB. To the extent that regional lung density is reflected by the water content, this then reflects perfusion in ml/min/g lung.

## Data Analysis

### Data representation

For each image acquired as described above (ASL perfusion, FLASH density, ASL/FLASH), the data were analyzed in the following manner. For each image, mean, standard deviation and relative dispersion (also know as the coefficient of variation, a global index of heterogeneity, defined as the standard deviation/mean where the larger the relative dispersion, the more heterogeneous the distribution) was calculated. The vertical distributions (distance above the most dependent portion of the lung for each subject) were plotted for each slice for perfusion (in ml/min/$cm^3$), density (g/$cm^3$) and perfusion normalized for density (ml/min/g). The relationship between vertical height and perfusion, density, and density normalized perfusion was characterized using least squares linear regression and the slope and strength of the association ($R^2$) obtained. Since distributions of perfusion and proton density across vertical distances may not necessarily be best expressed as a linear relationship, each sagittal slice was divided into three gravitationally-based regions of interest: dependent, middle, and non-dependent regions to allow for comparison between regions. The image with the greatest

anterior to posterior width was selected from the three contiguous sagittal images and divided horizontally into three regions of interest with equal vertical thickness based on the maximum A-P dimension of the lung. The remaining two contiguous lung slices were divided into three regions of interest using the same horizontal coordinates. Mean perfusion, density, and density normalized perfusion were obtained for each slice and region.

### Statistical analysis

Linear regression (Statview, 5.0 SAS Institute Inc. Cary, North Carolina) was used to evaluate the linear relationships between the vertical height and ASL perfusion, FLASH lung density, and density normalized perfusion (ASL/FLASH). These relationships were evaluated individually for each subject and the slopes of the relationships between vertical height and the variable of interest were evaluated using a one group t test comparing the means to zero. ANOVA for repeated measures was used to statistically evaluate changes in the major dependent variables over the three gravitational regions (3 levels: non-dependent, intermediate, dependent region). Dependent variables for this analysis were ASL measurement of perfusion in units of ml/min/cm$^3$ of lung, lung density as measured by FLASH in units of g/cm$^3$ lung, and ASL perfusion normalized for lung density (ASL/FLASH, ml/min/g). Where overall significance occurred, post hoc testing was conducted using Student's T testing. All data are presented as means ± SD, the null-hypothesis (no-effect) was rejected for $p < 0.05$, 2 tailed.

## RESULTS

### General Data

All subjects tolerated the study well. Heart rate averaged 66 ± 12 over the course of the study, and mean arterial oxygen saturation measured by pulse oximetry was 97.4 ± 1.0 %. The total duration of the study was approximately one hour.

### Lung Perfusion (ASL ml/min/cm$^3$)

Figure 1A shows the distribution of pulmonary perfusion (ml/min/cm$^3$ lung) from a middle lung slice in a representative subject lying supine in the MR scanner, after correction for coil heterogeneity. Lighter shades of gray denote greater flow. Figure 2A shows flow per voxel as a function of distance from the most dependent portion of the lung for all 3 slices in all 6 subjects, and Figure 2B shows the same data averaged for voxels lying within the same gravitational plane. Over all measurements, perfusion in the right lung averaged 1.7 ± 0.6 ml/min/cm$^3$. Perfusion heterogeneity, as measured by the relative dispersion (standard deviation of signal intensity/mean signal intensity) averaged 0.78 ± 0.23. This value is similar to that previously reported for healthy normal subjects of a similar age (18, 20, 27). There was a significant negative relationship between vertical height and perfusion for each subject and, on average, perfusion decreased by 3% per cm of height above the most posterior portion ($p < 0.0001$, Table 1). This slope was significantly different from zero ($p < 0.005$), however, the strength of the linear relationship, while statistically significant, was relatively weak (mean $R = 0.12$).

There was a highly significant difference ($p < 0.0001$) in perfusion between lung gravitational regions (Figure 2C). Lung perfusion was least in the non-dependent region (1.2 ± 0.5 ml/min/cm$^3$, significantly different from intermediate and dependent $p < 0.05$). However, lung perfusion averaged 1.9 ± 0.8 ml/min/cm$^3$ in the intermediate lung region, significantly ($p < 0.05$) greater than in either the non-dependent or dependent (1.7 ± 0.6 ml/min/cm$^3$) regions.

### Lung Density (Flash, g/cm$^3$)

Figure 1B shows lung density data measured with FLASH from the same middle lung slice in the same subject as in Figure 1A, after absolute quantification and correction for coil heterogeneity. Figure 2D shows density per voxel relative to mean density as a function of distance from the most dependent portion of the lung for all 3 slices in all 6 subjects, and Figure 2E shows the same data averaged for voxels lying with the same isogravitational plane. The density of right lung averaged 0.34 ± 0.08 g/cm$^3$. There was a highly significant negative relationship between height from the dependent portion of the lung and lung density ($p < 0.005$), with the density decreasing, on average, by 4.9 % per cm of height (Table 1). The strength of the linear association was much greater than for perfusion (average $R = 0.44$).

There was a highly significant difference ($P < 0.0001$) in density between lung gravitational regions such that density was significantly less in the non-dependent region and greater in the gravitationally dependent region (Figure 2F). In the non-dependent region, lung density averaged 0.28 ± 0.09 g/cm$^3$ and this progressively increased ($p < 0.05$) in the intermediate (0.33 ± 0.1 g/cm$^3$) and dependent (0.39 ± 0.09 g/cm$^3$) regions.

### Density Normalized Perfusion (ASL/FLASH, ml/min/g)

Figure 1C shows data from a middle lung slice in the same subject as in Figure 1 A and B after absolute quantification of perfusion and density, image registration, and division of the ASL measure of perfusion by the FLASH density to give a measure of perfusion per gram of lung (tissue + blood). Figure 2G shows density normalized perfusion graphed as a function of distance from the most dependent portion of the lung for all 3 slices in all 6 subjects. Figure 2H shows the same data averaged for voxels lying with the same isogravitational plane. Averaged over all measurements, the density normalized perfusion of the right lung averaged 5.12 ± 1.8 ml/min/g. There was no significant negative relationship between height from the most dependent lung region and perfusion when normalized for lung density, and averaged over all the six subjects, the slope of the linear relationship was not significantly different from zero ($p = 0.2$). However, there was a significant difference in density normalized perfusion between lung gravitational regions ($P < 0.05$, Figure 2I), with density normalized perfusion in the midzone of the lung being significantly greater than either the dependent or non-dependent regions. However in contrast to the ASL perfusion data, which was not normalized by density, the non-dependent lung regions did not differ significantly from the dependent lung regions.

## DISCUSSION

The results of this study indicate that *in situ* variations in regional lung density greatly affect the interpretation of data evaluating the gravitational gradients in pulmonary blood flow in the intact lung. The advantage of the techniques used in the present study is that both regional perfusion and lung density can be measured independently, allowing regional variation in lung density and *in situ* distortion of lung architecture to be accounted for. In our study, we found significant vertical gradients of perfusion, measured per cm$^3$ of lung, and lung density. However, when the regional variation in lung density was taken into account, these vertical gradients in perfusion were largely eliminated. These findings have important implications for reconciling differences between different measures of pulmonary perfusion which differ between *in situ* measurements, and microsphere measurements made *ex vivo*.

### Distribution of Perfusion and Density in the Lung

The lung presents unique challenges for the measurement of perfusion. In a tissue such as the brain, where the density is close to 1, the quantification of perfusion measured as ml/min/g tissue is not substantially different than perfusion measured by volume (ml/min/cm$^3$). Furthermore, the contribution of blood within the tissue to the overall density of the brain is

relatively small (about 4% (8)). However, in the lung the measurement of perfusion in ml/min/cm$^3$ gives very different values than the measurement of perfusion in ml/min/g tissue. This is because the lung density at functional residual capacity is approximately 1/3 of that of the brain and the blood volume itself contributes to more than one half of the weight of the lung (6). Further, lung density changes depending on the lung volume at which measurements are made (e.g. total lung capacity versus residual volume). In addition, any gravitationally based deformation of elastic structures with accompanying changes in regional lung density will influence the distribution of regional perfusion in a gravitationally dependent fashion. That the lung would deform under it's own weight was appreciated by West and Matthews more than 30 years ago, (47) as well as others (3,10,11). West and Matthews also pointed out that the regional differences in density would be accentuated by increased blood volume in the dependent portions of the lung. This concept was extended by Brudin et al. (6), who showed that the vascular component was the major contributor to vertical density gradients in the lung. Millar and Denison (36) expanded these observations by a theoretical analysis of computed tomography measures of lung density at different levels of lung inflation. They suggested that the lung behaved as a compressible foam, and that the vessels imposed an additional contribution to this density gradient. Recently, the effect that changes in posture have on the distribution of lung tissue were documented showing that the dependent lung tissue is compressed irrespective of prone or supine posture (38).

The data from the present study demonstrates the effect that these density gradients have on the interpretation of pulmonary perfusion measurements. Although in the 1960's, studies showed gravitational gradients in pulmonary ventilation and alveolar size (7,35) and numerous authors have referred to this mechanism and its effect on lung ventilation, what has been less-well appreciated is that this gravitational compression has direct and important effects on pulmonary perfusion. In essence, if one considers a lung that has perfectly uniform perfusion per alveolus, any effect that results in a gradient in alveolar size must necessarily result in a similar although reversed gradient in perfusion of the lung when viewed *in situ*, because the perfusion occurs within the walls of the alveoli. Conceptually, a simple analogy can be used: the lung might be thought of as a deformable structure like a "Slinky ®", (Figure 3) where the greater density of lung tissues in the dependent regions of the lung is analogous to a greater number of coils in the dependent portion of the spring when it is held in a vertical orientation. In this analogy, the pulmonary vessels form part of the coils and so a gradient in density also implies a gradient in overall perfusion. Using this analogy, it can be appreciated that measurements of perfusion in the intact lung will be influenced by this density distribution since measures made in the non-dependent portions will contain fewer blood vessels than in the dependent portions of the lung. In addition the contribution of the weight of the blood contained with the pulmonary vasculature is important because this has the potential to provide additional deformation of the elastic lung structures under the influence of gravity. These findings have important implications for how data are interpreted and compared between different techniques; measurements made *in situ* will be subject to the effects that lung density gradients have on perfusion whereas measurements made in excised lung will minimize these effects.

In this study, the spatial distribution of perfusion can be considered independently from the effects of changes in lung density. This can be appreciated by comparing Figure 2B to Figure 2H. Figure 2B shows a familiar pattern of blood flow that closely resembles the vertical perfusion gradients previously observed in data derived from a variety of sources (6, 22, 45). Perfusion is increased from non-dependent to dependent portions of the lung, and the presence of reduced perfusion in most dependent portion of the lung, the so called zone 4 region, is clearly visible. We found a vertical gradient in pulmonary perfusion (ml/min/cm$^3$) of 3% per centimeter, which is less than that reported for upright humans (~8% (3)), but which is comparable to that found in humans in the supine posture (~4%–5%, (1, 37)). We also observed

a vertical gradient in density of ~ 5% per cm in height (Figure 2D, 2E,2F), which is similar to that reported in the supine lung measured with SPECT (1) during quiet breathing and with computed tomography at residual volume (36), however the magnitude of this lung density gradient is less than reported by others (37) measured at different lung volumes. The effects of this vertical gradient in regional lung density can be seen in Figure 2H; the vertical gradient in perfusion is largely eliminated when normalized for regional density.

The implication of this observation is that a substantial part of the vertical gradient observed in perfusion in Figure 2A in the present study is a reflection of gravitationally-induced lung deformation as opposed to hydrostatic gradients in pulmonary vascular pressures. The extent of this can be expressed by the regression of perfusion and density, which yields a correlation of R = 0.40, thus approximately 20% of the observed regional variation in perfusion in our supine subjects at FRC can be explained by regional variation in density. This also suggests that when lungs are excised, washed of blood, air dried, and inflated to total lung capacity that vertical density gradients may be reduced. Thus we predict that if measured in supine humans at similar lung volumes and at a similar resolution, vertical gradients in blood flow measured by microspheres may more closely resemble the pattern in 2H.

## Effects of lung volume and supine posture on the gravitational influence on the distribution of pulmonary blood flow and density

A necessary limitation of magnetic resonance imaging is that most scanners can only accommodate recumbent postures for data collection. In upright postures, the gravitational influences are expected to be greater because the vertical height of the lung is greater, and thus both gravitational distortion and hydrostatic effects are greater. In addition, we imaged the lung at functional residual capacity as this improves the signal to noise characteristics of the ASL images obtained (31). However, the vertical gradients in regional perfusion are less at functional residual capacity than at total lung capacity (22). Thus, our data likely underestimate vertical influences in perfusion/$cm^3$ that might be found in the upright lung at total lung capacity. Nonetheless, the overall similarity between our data obtained at functional residual capacity and that using both radioisotopes, (22) and microspheres (12) is striking. It should be noted that the heterogeneity within plane and the lower $R^2$ for the relationship between height and perfusion in the present data is an expected consequence of the approximately one order of magnitude higher resolution of our MRI technique (about 0.14 $cm^3$) compared to microspheres (~1.2 $cm^3$), since greater variation in perfusion will be appreciated and, therefore, the standard deviation will be larger as the resolution of measurement increases. Vertical gradients in lung density have been shown to vary with lung volume, and in the supine posture, the density gradients at total lung capacity are less than those at residual volume (36). Thus depending on the conditions of measurement, including posture or lung volume, the net effect on lung density gradients and density normalized perfusion may be greater or less than identified by the current data.

It should be pointed out that our results do not exclude the presence of hydrostatically induced gradients in blood flow (the zone model, (45,46)) and the results in figure 2G–I are consistent with what might be expected in a normal supine human. Given the relatively anterior position of the heart in the chest, and typical pulmonary vascular pressures, one would expect most of the lung to be in zone 3, only a small zone 2 region, and in all likelihood, no zone 1. That is what is seen in figure 2H, where over much of the vertical extent of the lung, density normalized perfusion is quite uniform (in keeping with zone 3 conditions in which the arterial to venous pressure difference is constant). In the uppermost part of the lung density normalized perfusion falls with increasing height (consistent with zone 2 conditions). In the lowermost regions density normalized perfusion again decreases (consistent with zone 4 conditions (22)). In keeping with this idea, electron-beam computed tomography data obtained in the supine

posture and under positive pressure ventilation at a higher lung volume than the present study, where more zone 2 is likely, showed a persistent gradient in density normalized perfusion (23). However it is important to recognize that our measurements of lung density encompasses both the water containing portion of lung alveolar tissue and the blood in the pulmonary vasculature. Thus a region may have high density not only because of compression of the lung, but also because of a larger intravascular volume, and the relative contributions of these can not be distinguished from our data. In addition it is worth noting the high degree of perfusion heterogeneity within an isogravitational plane, and the low overall correlation between perfusion and vertical height, which is less than previously described for the mammalian lung (12,13) when evaluated at this high level of resolution. This suggests a substantial contribution from factors other than gravitational forces on the distribution of pulmonary blood flow.

## Technical limitations

MR imaging using ASL techniques has been widely used to determine regional blood flow in other organ systems, such as brain (8). The technique has been validated in tube-flow models (2), heart (40), brain (43) and skeletal muscle (42). However, there are some limitations to the technique that should be considered when evaluating our data. ASL-FAIRER provides an image map of all tagged protons that move into the imaging slice during the delay between tagging and image acquisition. Thus, components of both pulmonary arterial and venous blood flow are likely present, the significance of which is presently unclear (4). In addition, because the technique relies on a delay between tagging of protons and imaging, some slow moving tagged protons may not have entered the imaging plane. These theoretical considerations and a detailed description of the methods used in the present study to measure pulmonary perfusion and lung density including the advantages and disadvantages have been described in detail (4,16,21,44). Our measurement of perfusion for the right lung averaged 1.7 ml/min/cm$^3$, which is similar to values expected on theoretical grounds (4) and those measured using positron emission tomography (5), and MRI (4,44). Similarly, our density measurements are limited both by the need to correct for rapid signal loss in the lung (a short T2*, (17)) and by the extent that a small portion of the lung tissue may not generate MRI signal. Nevertheless, our density measurements are close to what might be expected. Since the weight of the human lung is about 1 kg including the blood in the pulmonary vasculature (6), the average density of the lung at functional residual capacity is expected to approximate 0.3 g/cm$^3$, and perfusion expressed per gram tissue is expected to be about 5 ml/min/gm. These values have also been confirmed by other studies (1,5,44) using a variety of techniques and are also remarkably close to the values for lung density of 0.34 g/cm$^3$ and perfusion per gram of 5.15 ml/min/g measured in the present study.

## Conclusion

The data in the present study suggest that *in situ* variations in regional lung density affect the interpretation of perfusion data in the lung. The vertical gradients in regional pulmonary perfusion are greatly reduced when normalized for regional variation in lung density, providing a means to reconcile the apparently discrepant results between microsphere and *in situ* data. A simple model, that the lung behaves like a Slinky®, a spring that deforms under its own weight, provides a simple conceptual model. Since it is already well-established that lung deformation due to gravity is present in the normal lung, and since the blood within the pulmonary vasculature forms a large proportion of the total lung weight with the potential to provide additional deformational forces under gravity, such effects need to be considered in the interpretation of regional measures of pulmonary perfusion.

### Acknowledgements

We would like to thank our subjects for their enthusiastic participation. This work was supported by NIH HL81171, NIH 1F32HL078128, and an Award from the American Heart Association (AHA 054002N).

## References


1. Almquist HM, Palmer J, Jonson B, Wollmer P. Pulmonary perfusion and density gradients in healthy volunteers. J Nucl Med 1997;38:962–966. [PubMed: 9189151]
2. Andersen IK, Sidaros K, Gesmara H, Rostrup E, Larsson HB. A model system for perfusion quantification using FAIR. Magn Reson Imaging 2000;18:565–574. [PubMed: 10913718]
3. Anthonisen NR, Milic-Emili J. Distribution of pulmonary perfusion in erect man. J Appl Physiol 1966;21:760–766. [PubMed: 5912745]
4. Bolar DS, Levin DL, Hopkins SR, Frank LF, Liu TT, Wong EC, Buxton RB. Quantification of regional pulmonary blood flow using ASL-FAIRER. Magn Reson Med 2006;55:1308–1317. [PubMed: 16680681]
5. Brudin LH, Rhodes CG, Valind SO, Jones T, Hughes JM. Interrelationships between regional blood flow, blood volume, and ventilation in supine humans. J Appl Physiol 1994;76:1205–1210. [PubMed: 8005864]
6. Brudin LH, Rhodes CG, Valind SO, Wollmer P, Hughes JM. Regional lung density and blood volume in nonsmoking and smoking subjects measured by PET. J Appl Physiol 1987;63:1324–1334. [PubMed: 3500940]
7. Bryan AC, Milic-Emili J, Pengelly D. Effect of gravity on the distribution of pulmonary ventilation. J Appl Physiol 1966;21:778–784. [PubMed: 5912747]
8. Buxton, R. Introduction to functional magnetic resonance imaging: principles and techniques. Cambridge, UK: Cambridge University Press; 2002.
9. Chang H, Lai-Fook SJ, Domino KB, Schimmel C, Hildebrandt J, Lee SC, Kao CC, Hsu JY, Robertson HT, Glenny RW, Hlastala MP. Redistribution of blood flow and lung volume between lungs in lateral decubitus postures during unilateral atelectasis and PEEP. Chin J Physiol 2006;49:83–95. [PubMed: 16830790]
10. Glazier JB, Hughes JM, Maloney JE, West JB. Measurements of capillary dimensions and blood volume in rapidly frozen lungs. J Appl Physiol 1969;26:65–76. [PubMed: 5762878]
11. Glazier JB, Hughes JM, Maloney JE, West JB. Vertical gradient of alveolar size in lungs of dogs frozen intact. J Appl Physiol 1967;23:694–705. [PubMed: 4862981]
12. Glenny RW, Bernard S, Robertson HT, Hlastala MP. Gravity is an important but secondary determinant of regional pulmonary blood flow in upright primates. J Appl Physiol 1999;86:623–632. [PubMed: 9931200]
13. Glenny RW, Lamm WJ, Albert RK, Robertson HT. Gravity is a minor determinant of pulmonary blood flow distribution. J Appl Physiol 1991;71:620–629. [PubMed: 1938736]
14. Glenny RW, Lamm WJ, Bernard SL, An D, Chornuk M, Pool SL, Wagner WW Jr, Hlastala MP, Robertson HT. Selected contribution: redistribution of pulmonary perfusion during weightlessness and increased gravity. J Appl Physiol 2000;89:1239–1248. [PubMed: 10956375]
15. Glenny RW, Polissar L, Robertson HT. Relative contribution of gravity to pulmonary perfusion heterogeneity. J Appl Physiol 1991;71:2449–2452. [PubMed: 1778945]
16. Haase A, Frahm J, Matthaei D, Haenicke W, Ferboldt K-D. Flash imaging: rapid NMR imaging using low flip - angle pulses. J Magn Reson 1986;67:258–266.
17. Hatabu H, Alsop DC, Listerud J, Bonnet M, Gefter WB. T2* and proton density measurement of normal human lung parenchyma using submillisecond echo time gradient echo magnetic resonance imaging. Eur J Radiol 1999;29:245–252. [PubMed: 10399610]
18. Henderson AC, Levin DL, Hopkins SR, Olfert IM, Buxton RB, Prisk GK. Steep head-down tilt has persisting effects on the distribution of pulmonary blood flow. J Appl Physiol 2006;101:583–589. [PubMed: 16601308]
19. Hlastala MP, Bernard SL, Erickson HH, Fedde MR, Gaughan EM, McMurphy R, Emery MJ, Polissar N, Glenny RW. Pulmonary blood flow distribution in standing horses is not dominated by gravity. J Appl Physiol 1996;81:1051–1061. [PubMed: 8889734]
20. Hopkins SR, Garg J, Bolar DS, Balouch J, Levin DL. Pulmonary blood flow heterogeneity during hypoxia and high-altitude pulmonary edema. Am J Respir Crit Care Med 2005;171:83–87. [PubMed: 15486339]

21. Hopkins SR, Levin DL, Emami K, Kadlecek S, Yu J, Ishii M, Rizi RR. Advances in Magnetic Resonance Imaging of Lung Physiology. J Appl Physiol 2007;102:1244–1254. [PubMed: 17158249]
22. Hughes JM, Glazier JB, Maloney JE, West JB. Effect of lung volume on the distribution of pulmonary blood flow in man. Respir Physiol 1968;4:58–72. [PubMed: 5639524]
23. Jones AT, Hansell DM, Evans TW. Pulmonary perfusion in supine and prone positions: an electron-beam computed tomography study. J Appl Physiol 2001;90:1342–1348. [PubMed: 11247933]
24. Kaneko K, Milic-Emili J, Dolovich MB, Dawson A, Bates DV. Regional distribution of ventilation and perfusion as a function of body position. J Appl Physiol 1966;21:767–777. [PubMed: 5912746]
25. Keilholz SD, Knight-Scott J, Christopher JM, Mai VM, Berr SS. Gravity-dependent perfusion of the lung demonstrated with the FAIRER arterial spin tagging method. Magn Reson Imaging 2001;19:929–935. [PubMed: 11595364]
26. Kosuda S, Kobayashi H, Kusano S. Change in regional pulmonary perfusion as a result of posture and lung volume assessed using technetium-99m macroaggregated albumin SPET. Eur J Nucl Med 2000;27:529–535. [PubMed: 10853808]
27. Levin DL, Buxton R, Spiess JR, Balouch J, Hopkins SR. Effects of Age on Regional Pulmonary Perfusion Heterogeneity Measured by Magnetic Resonance Imaging. J Appl Physiol. 2006under review
28. Lu H, Law M, Johnson G, Ge Y, van Zijl PC, Helpern JA. Novel approach to the measurement of absolute cerebral blood volume using vascular-space-occupancy magnetic resonance imaging. Magn Reson Med 2005;54:1403–1411. [PubMed: 16254955]
29. Maeda H, Itoh H, Ishii Y, Todo G, Mukai T, Fujita M, Kambara H, Kawai C, Torizuka K. Pulmonary blood flow distribution measured by radionuclide-computed tomography. J Appl Physiol 1983;54:225–233. [PubMed: 6600739]
30. Mai VM, Berr SS. MR perfusion imaging of pulmonary parenchyma using pulsed arterial spin labeling techniques: FAIRER and FAIR. J Magn Reson Imaging 1999;9:483–487. [PubMed: 10194721]
31. Mai VM, Chen Q, Bankier AA, Blake M, Hagspiel KD, Knight-Scott J, Berr SS, Edelman RR. Effect of lung inflation on arterial spin labeling signal in MR perfusion imaging of human lung. J Magn Reson Imaging 2001;13:954–959. [PubMed: 11382959]
32. Mai VM, Hagspiel KD, Christopher JM, Do HM, Altes T, Knight-Scott J, Stith AL, Maier T, Berr SS. Perfusion imaging of the human lung using flow-sensitive alternating inversion recovery with an extra radiofrequency pulse (FAIRER). Magn Reson Imaging 1999;17:355–361. [PubMed: 10195578]
33. Michels DB, Friedman PJ, West JB. Radiographic comparison of human lung shape during normal gravity and weightlessness. J Appl Physiol 1979;47:851–857. [PubMed: 511694]
34. Michels DB, West JB. Distribution of pulmonary ventilation and perfusion during short periods of weightlessness. J Appl Physiol 1978;45:987–998. [PubMed: 730604]
35. Milic-Emili J, Henderson JA, Dolovich MB, Trop D, Kaneko K. Regional distribution of inspired gas in the lung. J Appl Physiol 1966;21:749–759. [PubMed: 5912744]
36. Millar AB, Denison DM. Vertical gradients of lung density in healthy supine men. Thorax 1989;44:485–490. [PubMed: 2763259]
37. Musch G, Layfield JD, Harris RS, Melo MF, Winkler T, Callahan RJ, Fischman AJ, Venegas JG. Topographical distribution of pulmonary perfusion and ventilation, assessed by PET in supine and prone humans. J Appl Physiol 2002;93:1841–1851. [PubMed: 12381773]
38. Petersson J, Rohdin M, Sanchez-Crespo A, Nyren S, Jacobsson H, Larsson SA, Lindahl SG, Linnarsson D, Neradilek B, Polissar NL, Glenny RW, Mure M. Posture primarily affects lung tissue distribution with minor effect on blood flow and ventilation. Respir Physiol Neurobiol. 2006
39. Pluim JP, Maintz JB, Viergever MA. Mutual-information-based registration of medical images: a survey. IEEE Trans Med Imaging 2003;22:986–1004. [PubMed: 12906253]
40. Poncelet BP, Koelling TM, Schmidt CJ, Kwong KK, Reese TG, Ledden P, Kantor HL, Brady TJ, Weisskoff RM. Measurement of human myocardial perfusion by double-gated flow alternating inversion recovery EPI. Magn Reson Med 1999;41:510–519. [PubMed: 10204874]
41. Prisk GK, Guy HJ, Elliott AR, West JB. Inhomogeneity of pulmonary perfusion during sustained microgravity on SLS-1. J Appl Physiol 1994;76:1730–1738. [PubMed: 8045853]

42. Raynaud JS, Duteil S, Vaughan JT, Hennel F, Wary C, Leroy-Willig A, Carlier PG. Determination of skeletal muscle perfusion using arterial spin labeling NMRI: validation by comparison with venous occlusion plethysmography. Magn Reson Med 2001;46:305–311. [PubMed: 11477634]

43. Walsh EG, Minematsu K, Leppo J, Moore SC. Radioactive microsphere validation of a volume localized continuous saturation perfusion measurement. Magn Reson Med 1994;31:147–153. [PubMed: 8133750]

44. Wang T, Schultz G, Hebestreit H, Hebestreit A, Hahn D, Jakob PM. Quantitative perfusion mapping of the human lung using 1H spin labeling. J Magn Reson Imaging 2003;18:260–265. [PubMed: 12884340]

45. West JB, Dollery CT. Distribution of blood flow and ventilation-perfusion ratio in the lung, measured with radioactive carbon dioxide. J Appl Physiol 1960;15:405–410. [PubMed: 13844133]

46. West JB, Dollery CT, Naimark A. Distribution of Blood Flow in Isolated Lung; Relation to Vascular and Alveolar Pressures. J Appl Physiol 1964;19:713–724. [PubMed: 14195584]

47. West JB, Matthews FL. Stresses, strains, and surface pressures in the lung caused by its weight. J Appl Physiol 1972;32:332–345. [PubMed: 5010043]

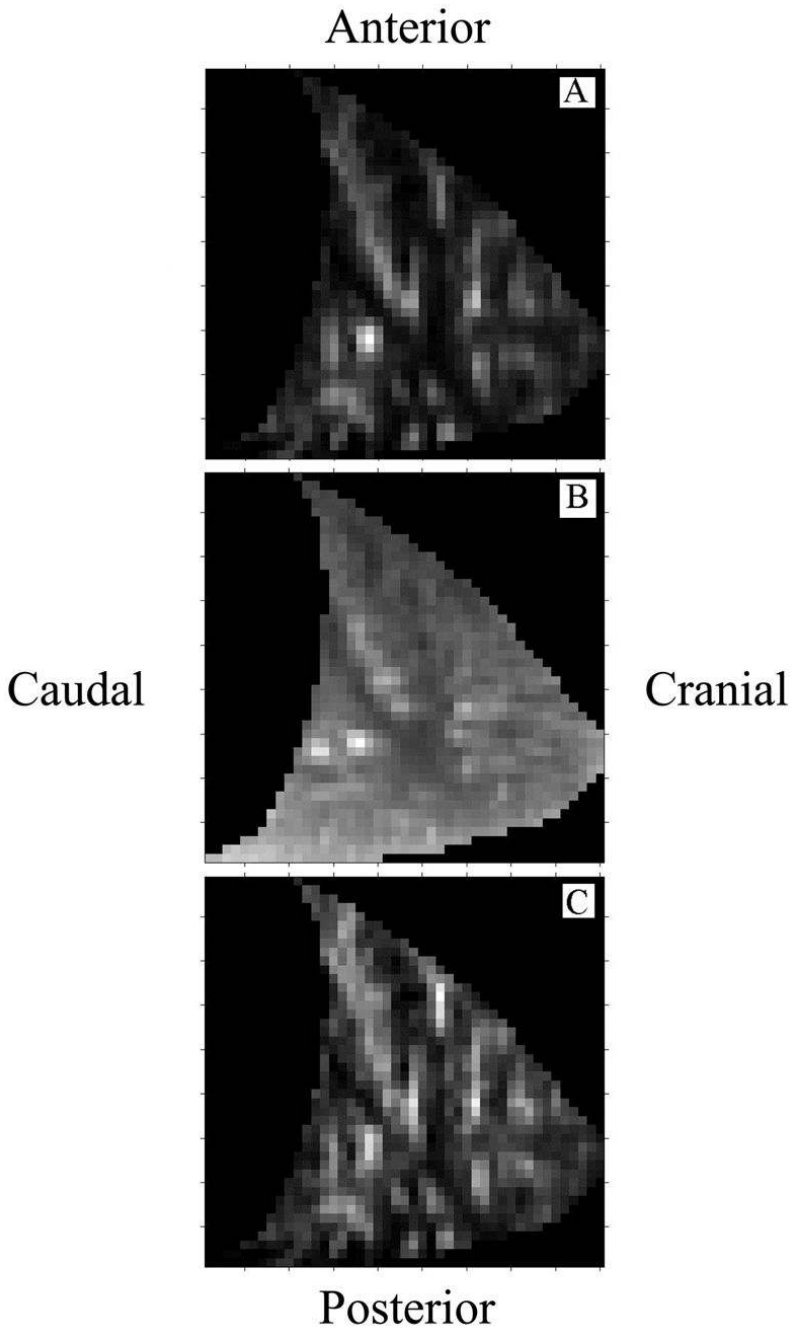


**Figure 1.**

Figure 1A shows an ASL measure of regional pulmonary blood flow (in ml/min/cm$^3$) after correction for coil heterogeneity and absolute quantification of perfusion in a representative subject lying supine in the MR scanner. This is a sagittal slice of the mid-right lung at functional residual capacity. The posterior lung is at the bottom of the image and region adjacent to the diaphragm is visible as the concave region on the left side of the image. The division of the right lung unto upper, middle and lower lobes is visible. The signal intensity of the images scales as a function of perfusion with brighter regions representing areas of greater blood flow. Figure 1B shows FLASH proton density (g/cm$^3$) measures of regional lung density in the lung same slice as Figure 1A. A vertical gradient in proton density is visible as brighter voxels in

the dependent portion of the lung. Figure 1C shows data from the same lung slice as Figure 1 A and B after absolute quantification of perfusion and density, image registration, and division of the ASL measure of perfusion by the FLASH density to give a measure of density normalized perfusion (ml/min/g).

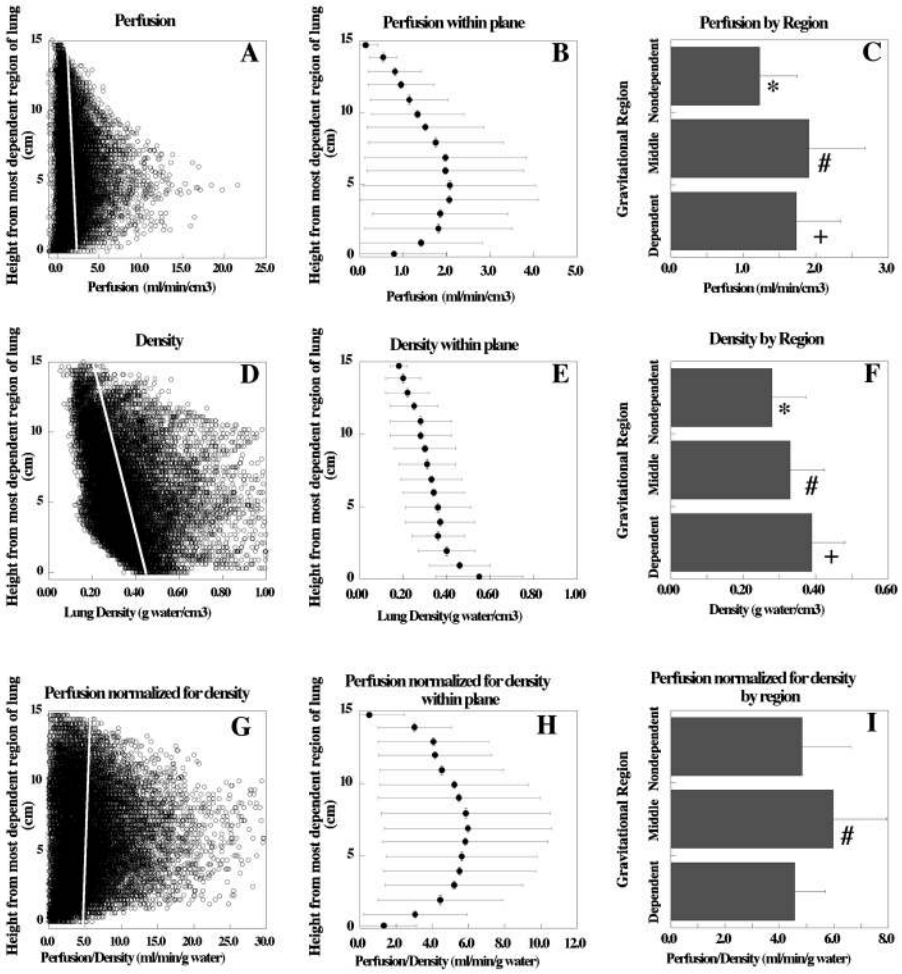


**Figure 2.**

The data in the left column in Figure 2 shows perfusion (A), density (D) and density normalized perfusion (G) per voxel graphed as a function of distance from the most dependent portion of the lung for all 3 lung slices in all 6 subjects. Note that the x and y axes have been reversed in the images so that vertical height increases up the figure. In each of these three figures the white line is the fit of the linear regression encompassing all data points. The middle column (B,E,H) shows the same data averaged for voxels lying within the same gravitational plane. The right hand column (C,F,I) shows the same data divided into 3 planes of equal height. It can be appreciated that the vertical slope in perfusion seen in Figure B is substantially altered when the significant vertical gradient in density (E) is accounted for, and in H the slope of the vertical relationship between density normalized perfusion and height is not significantly different from zero. Similarly, there was a significant difference in perfusion between lung gravitational regions (C) and perfusion was least in the non-dependent region and greatest in the intermediate lung region. Density was significantly less in the non-dependent region and greater in the gravitationally dependent region (F). When perfusion was normalized for density (I) perfusion in the middle region of the lung was significantly greater than either the dependent or non-dependent regions. However in contrast to the perfusion data which was not corrected for density (C), the non-dependent lung regions did not differ significantly from the dependent lung regions. (see text for details). * = significantly different from middle and dependent region, # = significantly different from dependent and non-dependent region, + = significantly different from non-dependent and middle region, all $p < 0.05$.

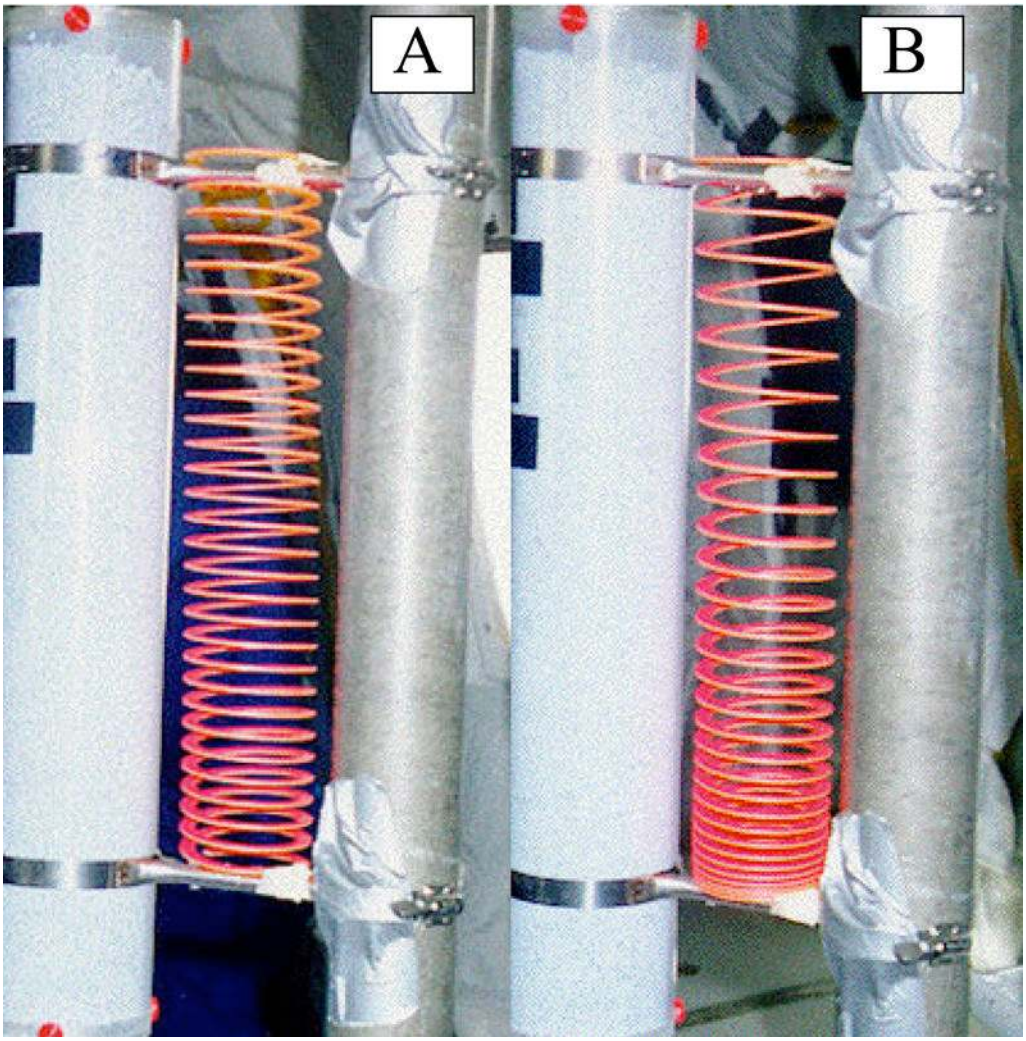


**Figure 3.**
A Slinky®-type deformable spring during parabolic flight. In A, taken in zero G, the coils of the spring are uniform, whereas in B taken in 2 G the effects of gravity on the distribution of the coils are clearly visible.

**Table 1**

Slope and degree of association for the relationship of perfusion and Density in the lung to vertical distance from the most dependent lung region.

| Subject | Perfusion Slope (%/cm) | R | Density Slope (%/cm) | R | Density Normalized Perfusion Slope (%/cm) | R |
|---|---|---|---|---|---|---|
| 1 | −3.1 | 0.13 | −5.8 | 0.41 | +2.2 | 0.13 |
| 2 | −2.1 | 0.06 | −4.6 | 0.41 | +1.3 | 0.04 |
| 3 | −3.8 | 0.10 | −1.2 | 0.09 | −2.6 | 0.08 |
| 4 | −4.4 | 0.22 | −5.8 | 0.63 | +1.4 | 0.08 |
| 5 | −1.5 | 0.06 | −6.3 | 0.57 | +3.6 | 0.16 |
| 6 | −2.8 | 0.13 | −5.8 | 0.54 | +2.4 | 0.11 |
| Mean | −3.0 | 0.12 | −4.9 | 0.44 | +1.4 | 0.10 |
| SD | ±1.1 | ±0.06 | ±1.9 | ±0.19 | ±2.1 | ±0.04 |
| P | <0.005 | | <0.005 | | 0.2 | |

The P value is the result of one group t-test comparing means to zero.